https://doi.org/10.15623/ijret.2018.0702008 Received: 29-12-2017, Accepted: 08-02-2018, Published: 28-02-2018

DOCKING AND SPECTRAL INVESTIGATIONS (FT-IR, FT-Raman, NMR, UV-Vis) ON 7-Hydroxyl-4-Chromone USING QUANTUM COMPUTATIONAL (DFT) ANALYSIS

K. Jayasheela[1], S. Periandy[2], S.Xavier[3], K. Niveditha[4]

[1]*Department of Physics, Kanchi mamunivar Centre for Postgraduate Studies, Puducherry, India*
[2]*Department of Physics, Kanchi mamunivar Centre for Postgraduate Studies, Puducherry, India*
[3]*Assistant Professor, Department of Physics, St. Joseph's arts and Science college, Cuddalore, India*
[4]*Department of Physics, Kanchi mamunivar Centre for Postgraduate Studies, Puducherry, India*

Abstract

Vibrational analysis of 7-hydroxy-4-chromone is carried out by using FT-IR and FT-Raman spectroscopic techniques. Gaussian computational calculations were performed using B3LYP method with 6-311++G (d, p) basis set. The results reveal that the lone pair transition has higher stabilization energy compared to all other atoms. The ^{1}H and ^{13}C NMR chemical shifts are calculated using the Gauge-Including Atomic Orbital (GIAO) functional along with B3LYP/6-311++G (d, p). The study on the electronic and optical properties; absorption wavelength, frontier molecular orbital and Molecular electrostatic potential (MEP) exhibit the high reactivity nature of the molecule. The docking study shows the antimutagenic activity in E.coliinosine triphospate pyrophoshatase RgdB in comples with IMP anthracis protein.

Keywords: *Docking, FT-IR, FT-RAMAN, NMR, UV-vis*

----------***----------

1. INTRODUCTION

7-hydroxy-4-Chromone is occurring naturally in soybean and are also found in plants that humans generally do not eat such as red clover [1] consists of two benzene rings; one of it is an oxygen substituted heterocyclic ring, while the other one is attached with a hydroxyl group. Functions including antioxidant, anti-inflammatory, cell cycle arrest and biological activities in humans. The antioxidant effect has been demonstrated in many biologically relevant systems [2]. Chromone has been observed in naturally occurring pharmotherapeutic compounds. These compounds have important health protecting properties such as antioxidant, anti-inflammatory, anti-allergic, anti-bacterial, anti-parasitic, anti-fungal, antimicrobial, anti-diabetic and anti-carcinogenic properties [3].

Chromone and their structural activities in specify behaviour on against oxidation processes. This compound is the most motivated great interest within the medicinal chemistry field and bio active molecules. Molecule behaviour in acid-base profile and character interact with biochemical reaction. Therefore, the molecule in activity of photochemical relies on their structural prevent, the namely the phenolic OH groups. In the present study, a series of chromone based compounds with different ring substitution patterns are assessed as their free radical ability in order to assume the optimal molecular features associated with this antiradical activity [4]. There were so many studies have been carried and reported [1-11], but spectroscopic studies with the special comparison the quantum computational methods have not yet been reported so far. This present study is aimed at making analytical comparison of the spectroscopic data with the theoretical studies.

2. EXPERIMENTAL DETAILS AND COMPUTATIONAL METHODS

The compound under investigation 7-hydroxy-4-chromone was purchased in powder form from Sigma-Aldrich chemicals, Chennai. The FT-Raman spectrum of 7-hydroxy-4-chromone was recorded using Nd-YAG laser at 1064 nm wavelength in the region 500-3500 cm^{-1} . The sample was prepared using KBr pellet technique because of solid state. The FT-IR spectrum of a molecule recorded in the region 500-4000cm^{-1} using IFS 66V spectrophotometer in Annamalai University, Chidambaram. The UV-Visible spectrum was recorded in liquid phase dissolved in di-methyl sulphoxide (DMSO) in the range of 200-400 nm, with the scanning interval of 0.2nm, using the UV-1700 series instrument in Pondicherry University. The NMR spectrum was recorded in liquid phase dissolved in DMSO in the range of 20-200 ppm with the scanning interval of 20 ppm in Pondicherry University.

All the quantum chemical computations in the present work are performed using the Gaussian 09 software programs [12] on a Pentium IV/3.02GHz personal computer. The geometrical parameters and vibrational were computed using B3LYP methods with 6-311++G (d, p) basis set. The UV-Visible spectra electronic transition such as HOMO-

https://doi.org/10.15623/ijret.2018.0702008 Received: 29-12-2017, Accepted: 08-02-2018, Published: 28-02-2018

LUMO excitation energies and oscillator strength were calculated using time-dependent TD-SCF-B3LYP method using experimental also. The NMR chemical shift was carried out by GIAO method in B3LYP method with 6-311G++ (d, p) basis set [56]. The natural bonding orbital (NBO) computations were done using B3LYP function with 6-311+G (d, p) basis set level a second-order perturbation theory.

3. RESULT AND DISCUSSION

3.1 Conformational Analysis

The 7-hydroxy-4-chromone has hydroxyl and pyrone substituent groups attached to a benzene ring. The conformational analysis of the molecule 7-hydroxy-4-chromone was performed using B3LYP/6-311++G(d,p) method [13], by potential energy surface scan technique, by varying the dihedral angle C2-C1-O17-H18 in steps of 10^0 for a complete rotation 0-360^0 [14]. The result of the scanning is shown graphically in Fig. 1. which clearly shows that there are two minimum at 0^0 and 360^0 with energy -0.1274 Hartree. Hence, these conformers both of them are structurally identical, serve as the most stable conformer of the compound. There are two maximum energy points also at 59.42^0 and 308.57^0 with energy value -0.119 Hartree, which are the least stable conformers of the compound.

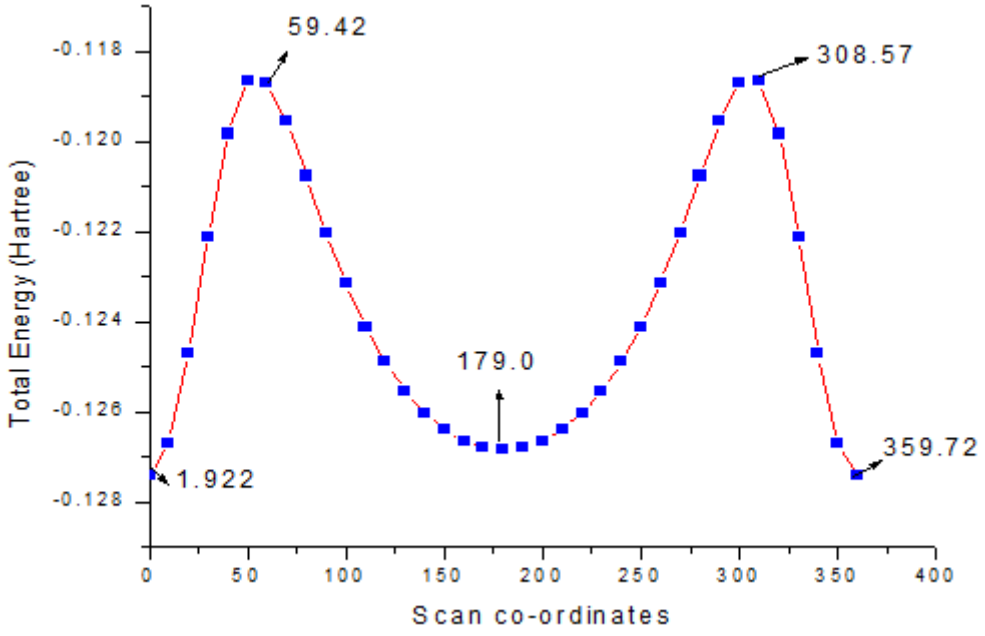

Fig 1: The potential energy curve of 7-hydroxy 4-chromone

3.2 Structural Analysis

The structural analysis of 7-hydroxy-4-chromone was carried out using B3LYP method with 6-311+G(d,p) and 6-311++G(d,p) basis sets [12], for the optimized geometry of the most stable conformer of the compound. The bond length and bond angles calculated using these methods are presented in Table 1. From the geometry of the compound, it is clear that there are nine C–C, five C–H, four C-O and one O-H bonds. According to previous work [14], the bond length for CC single bond is expected to be around 1.46 Å and that of CC double bond around 1.34 Å. In the present molecule, the bond length for CC in the benzene ring is observed between 1.37-1.39 Å.

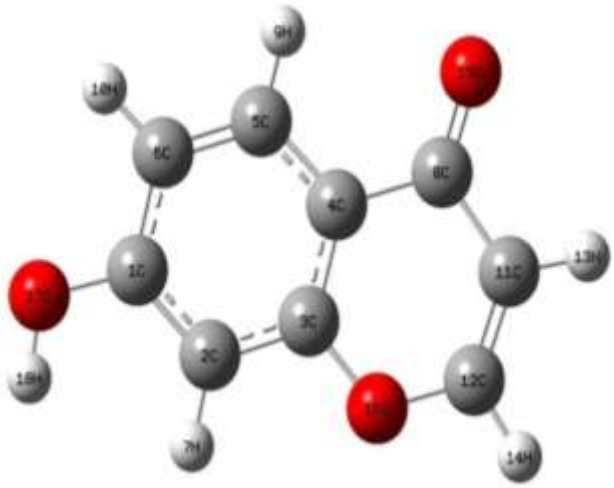

Fig 2: Molecular structure of 7-hydroxy 4-chromone

https://doi.org/10.15623/ijret.2018.0702008 Received: 29-12-2017, Accepted: 08-02-2018, Published: 28-02-2018

This shows that the bonds present inside the benzene ring is neither double bond nor single bond and all the bonds have some intermediate values, which is in agreement with an earlier work on benzene derivative [15], this may be due to the conjugation of the electrons inside the benzene ring which leads to almost equal distribution of electron density between the double and single bonds.

The slight variation among the CC bond length within the benzene ring is due to the substitutional groups; the OH group at C1 position and pyrone ring fused at C4 and C3. The bond length C3–C4 is observed to be 1.39Å in all the computational method, agreeing with the experimental value [5, 16]. The bond length for C1-C6 and C4-C5 are observed to be 1.40Å. These slight increases in bond length may be due to the presence of oxygen atoms at C1 and C8 respectively. The CC bonds in the pyrone ring show that the bond length for C4-C8 and C8-C11 are 1.46Å, which means they are purely single bond, while the bond C11-C12 is 1.34Å which is purely double bond [5]. This variation of bond lengths with respect to the benzene ring shows that there is no such conjugation of electrons in this pyrone ring as it is in the benzene ring, which may be due to the presence of two oxygen atoms O13 and O15 in this ring.

When the CO bonds in the molecule are compared, it is found that C8-O15 bond length is 1.22Å and that of C1-O17 is 1.36 Å. This difference in length clearly indicates that C1-O17 is a single bonded C-O whereas C8=O15 is double bonded [16]. Both of these bonds are present outside the rings, hence the influence on these bond lengths may not be significant. The other C-O values are 1.37 and 1.35Å for C3-O16 and C12-O16 respectively, which is slightly high and low to the C-O single bond present in hydroxyl group. The difference between these two values is found to be due to the attachment of pyrone ring with the benzene ring at C3-C4 single bond and the presence of double bond C11-C12 adjacent to these bonds. All the C-H bonds are expected to be un-influenced due to their presence outside the rings, in this molecule also this trend is observed and the C-H single bonds are having the same values around 1.08 Å [17], irrespective of whether they are present in the benzene ring or in the pyrone ring. This shows clearly the presence of oxygen atoms in both ringhas not influenced the CH bond lengths.

The bond angles around each carbon atom, in both benzene and pyrone rings are expected to be 120^0 due to sp^2 hybridization [5]. In this molecules the bond angles at C2-C1-C6and C3-C4-C8 are observed to be 120^0 as expected, but other bond angles varies between 117^0 to 122^0, which shows that the bond angles are deviated from the expected value, these are again due to the presence of oxygen atoms in both benzene and pyrone rings, which disturbed the electronic conjugation in both rings, though it is less in benzene ring and high in pyrone ring. The same 120^0 angles is expected for all C-C-H single bonds also, but a similar variation in the bond angles are also observed for this C-C-H single bonds, which is also due to the variation of the electronic conjugation among the C-C-C single bonds, due to the presence of oxygen atom . These entire C-C-C and C-C-H bond angle values also indicate that both benzene and pyrone rings are slightly distorted due to the amalgamation of the two rings and the presence of oxygen atoms.

Table 1: Optimized Geometrical parameter for 7-Hydroxy-4-Chromone

Parameters Bond length (Å)	**B3LYP/ 6-311++G(d,p)**	**XRD (Bond length)**	**Parameters Bond Angle(°)**	**B3LYP/ 6-311++G(d,p)**	**XRD (Bond Angle)**
C1-C2	1.389	1.375	C2-C1-C6	120.6	120.7
C5-C6	1.378	1.381	C1-C2-C3	118.6	119.0
C2-C3	1.395	1.400	C2-C3-C4	122.0	121.4
C3-C4	1.399	1.397	C3-C4-C5	117.7	118.5
C1-C6	1.406	1.407	C4-C5-C6	121.3	120.5
C4-C5	1.406	1.403	C1-C6-C5	119.5	119.9
C4-C8	1.477	1.468	C3-C4-C8	120.4	119.8
C8-C11	1.464	1.455	C5-C4-C8	121.8	121.7
C11-C12	1.342	1.346	C4-C8-C11	113.4	121.3
C6-H10	1.082	0.950	C8-C11-C12	121.2	119.4
C5-H9	1.083	0.950	C1-C2-H7	121.9	120.5
C2-H7	1.084	0.950	C3-C2-H7	119.4	120.5
C11-H13	1.082	0.950	C4-C5-H9	117.5	119.8
C12-H14	1.082	0.950	C6-C5-H9	121.0	11*9.7
C8-O15	1.225	1.236	C1-C6-H10	118.7	120.0
C3-O16	1.371	1.370	C5-C6-H10	121.6	120.1
C12-O16	1.354	1.352	C8-C11-H13	118.8	119.7
C1-O17	1.361	1.429	C12-C11-H13	119.9	119.7
O17-H18	0.963	0.840	C11-C12-H14	124.7	117.2
			C4-C8-O15	123.2	121.3
			C11-C8-O15	123.2	123.5

https://doi.org/10.15623/ijret.2018.0702008 Received: 29-12-2017, Accepted: 08-02-2018, Published: 28-02-2018

			C2-C3-O16	116.1	116.7
			C4-C3-O16	121.8	121.9
			C11-C12-O16	124.5	125.6
			H14-C12-O16	110.7	117.2
			C3-O16-C12	118.5	118.0
			C6-C1-O17	116.7	
			C1-O17-H18	110.3	

3.3 NMR Analysis

NMR spectroscopy has proven to be an exceptional tool to elucidate the information about the structure and reaction ability of the molecules. To provide an explicit assignment and analysis of ^{13}C and ^{1}H NMR spectra, experimental and theoretical chemical shift of the title compound are determined. The computational shifts were determined using gauge independent atomic orbital (GIAO) functional along with B3LYP functional and 6-311+G (2d, p) basis set combination [18, 19], the calculations were performed both in gas as well as in DMSO solvent phases. The experimental and theoretical ^{13}C NMR and ^{1}H chemical shift values are presented in Table .3 and the corresponding theoretical and experimental spectra are presented in Fig. 4 and Fig. 5 respectively.

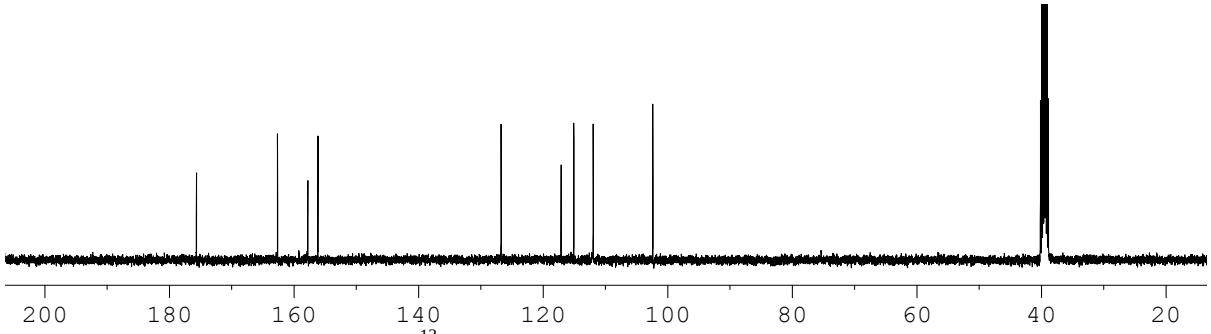

Fig 4: Experimental ^{13}C NMR spectrum (DMSO) of 7-hydroxy 4-chromone

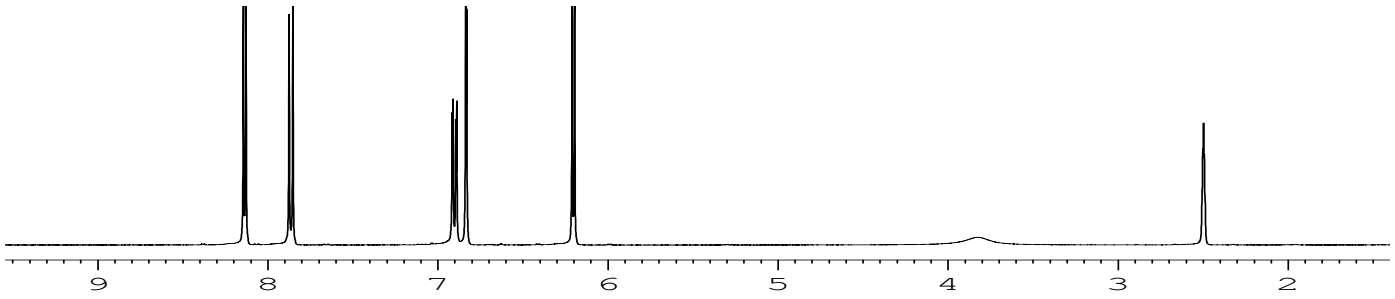

Fig 5: Experimental ^{1}H NMR spectrum (DMSO) of 7-hydroxy 4-chromone

Aromatic carbons give signals with chemical shift values from 120 -130 ppm [63]. This observation is made only in few carbon atoms in this molecule. The chemical shift of C2, C4, C5, C6 atoms in benzene ring shows the value of aromatic carbon atoms. The C1 and C3 values are slightly greater than the expected values, which may be due to the presence of O atom with C3 and double bond between C2=C3. Thus, the conjugation of electrons is not uniform within this benzene ring which deviates much in the region C1-C2-C3. The chemical shift values for carbon atoms in the pyrone ring are found to be C8-175.67, C11- 117.11 and C12- 156.16 ppm. These values are relatively larger except for C11 when compared to benzene ring which clearly shows the electronic conjugation in this ring is entirely different from that of benzene, which was also identified in structural analysis. The reason for large value of C8 & C12 which lies within the ring may be due to its attachments with oxygen atoms; hence they are highly positive in charge which produces a large shift in the values. C1 which lies in the hydroxyl group has equally large shift which is due to the presence of Oxygen atom. The NAC methods of charge distribution among these carbon atoms support these chemical shift values.

The chemical shift values for H atoms attached to benzene ring are expected between 7-8 ppm. Here for these H atoms, the values are 6.9, 8.1, 6.8, 6.2, 7.8 ppm, all these values are except values. There is only two 18H atom in very low range 2.5 because the intermolecular hydrogen bonds are present in the molecules. The computed chemical shifts in

https://doi.org/10.15623/ijret.2018.0702008 Received: 29-12-2017, Accepted: 08-02-2018, Published: 28-02-2018

gas & DMSO phases indicate that the chemical shift values are relatively higher in solvent phase when compared to gas phase.

Table 3: Calculated ^{1}H and ^{13}C NMR Chemical shifts (ppm) of 7-Hydroxy-4-Chromone

Atom	B3LYP/6-311++G(d,p) GIAO (ppm) (Gas)	B3LYP/6-311++G(2d,p) GIAO (ppm) (DMSO)	Experimental (DMSO)
1C	166.36	168.18	162.65
2C	103.55	106.26	102.39
3C	163.63	165.15	157.16
4C	125.23	124.57	111.97
5C	135.13	132.59	115.08
6C	117.58	134.58	126.75
8C	177.15	181.61	175.67
11C	119.33	135.03	117.11
12C	158.10	162.81	156.16
7H	6.4798	7.3052	6.914
9H	8.3821	8.5932	8.147
10H	7.0429	7.4661	6.839
13H	6.1379	6.6226	6.213
14H	7.5315	8.2548	7.856
18H	4.4128	5.5500	2.504

3.4 Vibrational Analysis

The title molecule 7-hydroxy-4-chromone has 18 atoms and it belongs to C_1 point group symmetry. The maximum number of fundamental modes of vibrations for the non-linear molecule can be calculated from the relation (3N-6), where N is the number of atoms present in the molecule, where 6 represents three translational and three rotational degrees of freedom. Hence the title molecule has 48 possible modes of vibrations [20]. All these modes of vibrations are observed collectively in both IR and Raman spectra. The wave numbers are calculated using B3LYP functions with the 6-311++G (d, p) basis set and the assignments are made based on total energy distribution (TED) values, all these values are presented in Table 4. The experimental spectra, FT-IR and FT-Raman recorded for the title molecule are presented in Fig. 6 & Fig. 7 respectively.

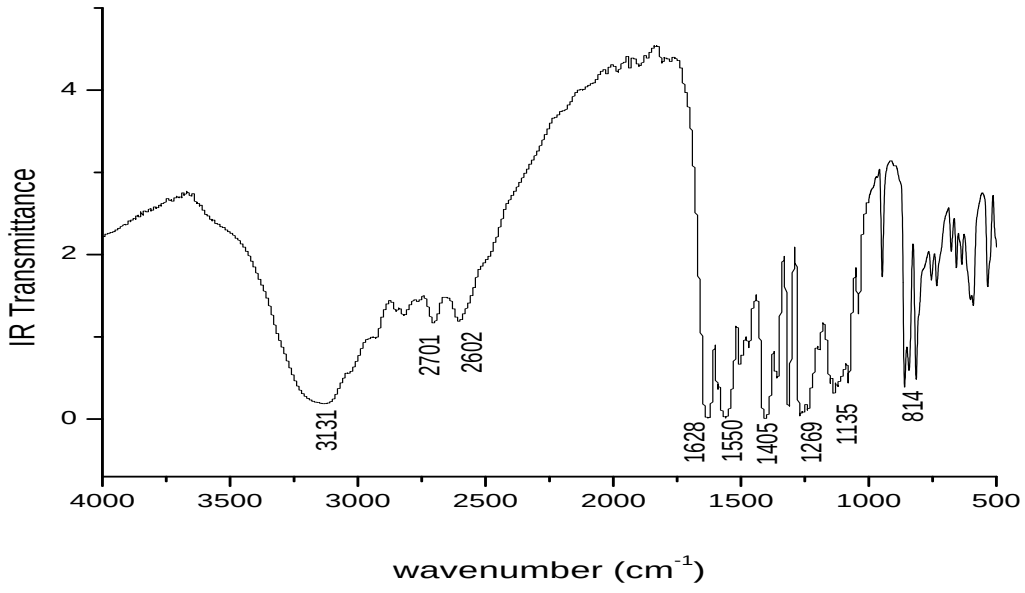

Fig 6: Experimental FT-IR spectra of 7-hydroxy 4-chromone

https://doi.org/10.15623/ijret.2018.0702008 Received: 29-12-2017, Accepted: 08-02-2018, Published: 28-02-2018

OH Vibrations

There is single OH group attached with pyrone rings, the stretching vibration due to these band expected to be in the range of 3700 – 3300 cm^{-1} [21, 22]. The OH group vibration are likely to be the most sensitive to the environment, so they show pronounced shifts in the spectra of the hydrogen bonded species. The band corresponding to OH stretching in this molecule is not clear peak because intermolecular hydrogen bondings are present. This wave number observed for OH indicates that this OH involve in hydrogen bond formation, as the values are found at the higher end of the expected region. The scaled value computed using B3LYP function with 6-311++G (d,p) basis set lie closer to the experimental values which has difference of ~ 10 cm^{-1}. The same trend is observed in literature also [23].

OH in-plane bending band is expected at 1451cm^{-1} [23], this is observed at 1456 cm^{-1} in FT-Raman spectra in the present molecule. Similarly, the out of plane bending modes are expected between 710 – 517 cm^{-1}, but this is observed at 839 cm^{-1} in the present case. This deviation is generally expected at the out of plane bending modes, as the interaction between various modes at this lower range is very stronger, the bands are very close to each other at these ranges.

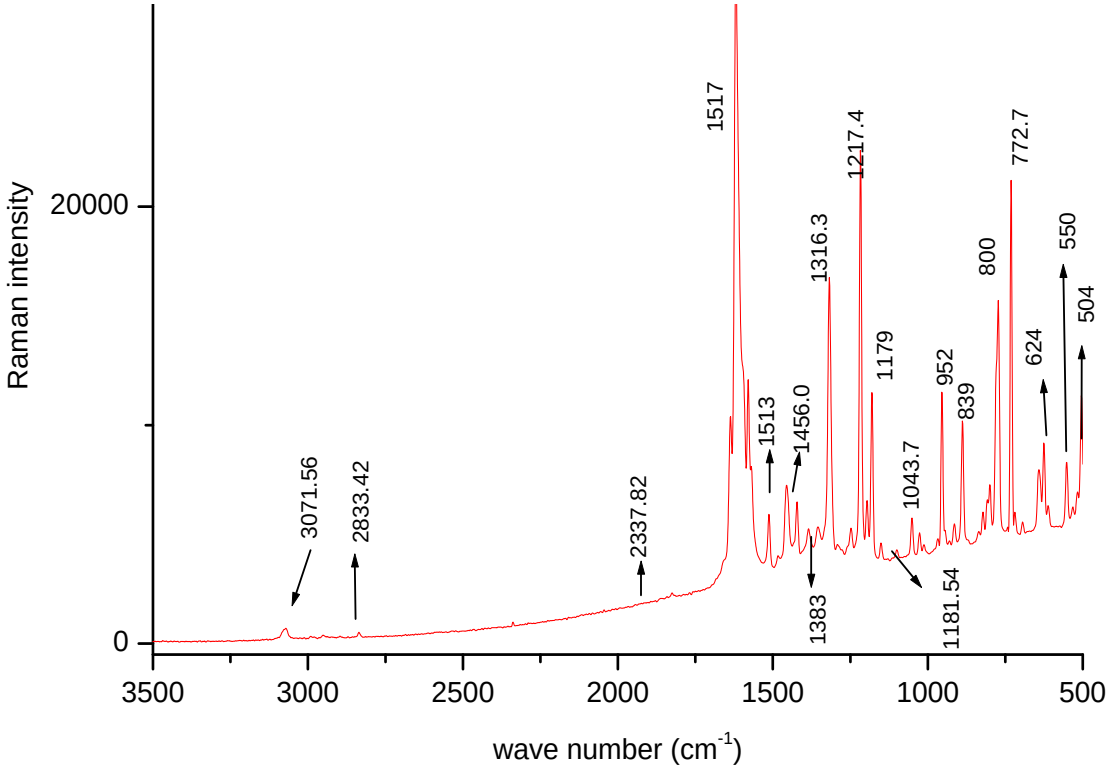

Fig 7: Experimental FT-Raman spectra of 7-hydroxy 4-chromone

C-H Vibrations

For all the aromatic compounds the carbon-hydrogen stretching vibrations are expected in the region 3100–3000 cm^{-1} and for aliphatic compounds in the region 3000–2900 cm^{-1} [24]. In the present study, there are five CH stretching vibrations, in which three belong to benzene ring and the rest belong to pyrone ring. The CH stretching bands which belong to ring are observed at 3131, 3071, 2833, 2701, 2602 cm^{-1}. This observation indicates that the electronic distribution or conjugation within the rings is different in both these rings than that of pure benzene ring.

The CH in-plane bending and CH out-of-plane bending vibrations are expected in the range 1300 -1000 cm^{-1} and 1000 - 750 cm^{-1}, respectively for benzene derivatives [25, 26]. In the present case, the in-plane bending bands of benzene and pyrone CH are observed at 1135, 1181, 1076, 1043 and 1036 cm^{-1}. All these values are lesser than the expected range. The out–of- plane bending vibrations of the benzene and pyrone are observed at 947, 952, 814, 800, 752 cm^{-1} in FT-IR and FT-Raman. The TED values show that these modes are mixed with CC and CO bands. Hence, the presence of too many C-O and CC modes in this molecule, which also lie in this range, has pushed down the bending vibrations below the expected range, due to the Fermi resonance effect. The computed values are found closer to the observed values.

C=C, C-C Vibrations

For benzene derivatives, the CC double bond and CC single bond stretching vibrations, known as semicircle stretching of hexagonal structure, usually observed in the region of 1650

https://doi.org/10.15623/ijret.2018.0702008 Received: 29-12-2017, Accepted: 08-02-2018, Published: 28-02-2018

to 1500 and 1500 to 1400 cm^{-1} [26] respectively. Though, there used to be no clear cut demarcation between single and double bond within the ring, the higher part of the region is usually assigned to CC double bond stretching modes and the lower part to CC single bond. The presence of conjugation within the ring causes a heavy doublet formation around the region 1625 and 1575 cm^{-1}.

In present study, the CC double bond stretching is observed at 1517, 1405, 1456, 1356 cm^{-1}. The CC single bond stretching vibrations are observed at 1313, 1269, 1236, 1217, 1179cm^{-1}. According to the structure, there is one double bond CC clearly, so 1517 must be due to this bond, which shows the pyrone ring is less aromatic. The other three values of benzene ring 1405, 1456, 1356 cm^{-1} shows these bonds are closer to single bond. All the single bond values are less than the expected values both for benzene and pyrone rings, except the first two bands. This decrease in values is also due to the presence of CO modes in this molecule which is also ascertained by TED values.

C=O, C-O Vibrations

For benzene derivatives, the CO double bond and CO single bond stretching vibrations, known as semicircle stretching of hexagonal structure, are usually observed around 1750–1500 cm^{-1} [26]. The Stretching vibration for this CO double bond in the present case is observed at 1758, 1711, 1628, 1550, 1517 cm^{-1} in both FT-IR and FT-Raman. The stretching modes of the C-O bonds are expected around 1150-1450 cm^{-1}. In the present case, the stretching vibrations for these CO single bond are observed at 1200, 1153, 1135, 1269, 1082 cm^{-1} in both FT-IR and FT-Raman. All these bonds are present within the pyrone ring, and they almost close to the expected values, which indicate these bands are not much influenced by the Ketone group present with this ring.

Table 4: Observed method DFT (B3LYP) with 6-311++G (d,p) level calculated vibrational frequencies of 7-hydroxy-4-chromone.

Symmetry species (Cs)	Experimental frequency(cm^{-1})		B3LYP/6-311++G	Assignment	VED%
	FT-IR	FT-Raman	Scaled (cm^{-1})		
A'	3652v		3818	ν OH	ν OH (100)
A'			3204	ν CH	ν CH (99)
A'			3188	ν CH	ν CH (62)
A'			3186	ν CH	ν CH (77)
A'	3131s		3176	ν CH	ν CH (38)
A'		3071vw	3105	ν CH	ν CH (99)
A'			1705	ν C=O	ν OC (34) + ν CC (12)
A'			1654	ν C-O	ν CC (26) + ν CC (11)
A'	1628s		1633	ν C-O	ν CC (15) + ν OC (37)
A'	1550s		1614	ν C-O	ν CC (32) + β HCO10
A'		1517vs	1543	ν C=C	ν CC (11) + β HCC(14)
A'			1498	ν C=C	ν CC (12) + β HOC(18) + β HCC(14)
A'	1405s	1456w	1456	ν C=C	ν C=C (10) + β HCC (22) + β HCO (36)
A'		1383vw	1392	ν C=C	β HCC(16) + β HOC(20)
A'	1356s		1387	ν C-C	ν CC (14) + β HOC(33)+ β HCC(11)
A'	1313s	1316s	1316	ν C-C	ν CC (10) + ν OC (14)
A'	1269s		1278	ν C-C	ν OC (25)+ β HCC(26)
A'	1236s	1217vs	1248	ν C-C	ν OC (12)+ β HCC(19) + β HCO(11)
A'		1179s	1181	ν C-C	ν CC (11)+ β HCC(19)
A'	1170s		1159	β OH	ν CC (22)+β HCC(34)
A'	1135w	1181w	1128	β CH	ν CC (15)+β HCC(47)
A'	1076m	1043w	1069	β CH	β CCC(17)
A"	1036w		1037	β CH	δ HCCC(59) + δ CCCC(16)
A"			997	β CH	δ HCCO(16) + δ HCOC(61)
A'	947w	952vw	956	β CH	ν OC (32)+ ν CC(10)
A'			941	β C=O	ν OC (13)+β CCC(29)
A"	859s		875	β C-O	δ HCCC(46) + δ OCCC(15)

https://doi.org/10.15623/ijret.2018.0702008 Received: 29-12-2017, Accepted: 08-02-2018, Published: 28-02-2018

A"	839m	839s	865	δ OH	δ HCCC(47) + δ OCCC(11)
A"			830	δ CH	δ HCCO(55) + δ HCOC(12) + δ O CCC (22)
A'	814m	800s	805	δ CH	ν CC (16)+β CCO(16)
A"			750	δ CH	δ HCCO(21)
A'	752w		745	δ CH	ν CC (20)+β CCC(16)
A"			709	δ CH	δ HCCC(14) + δ CCCC(32)
A"	625w	624vw	635	δ C-O	δ OC(12))+β COC(15)+β CCO(13)
A"	590s		543	β COH	δ HOCC(13) + δ OCCC(27)
A"	533w		538	β CCC	δ HOCC(83)
A"			488	β CCC	δ CC(14) + β OCC(14)
A'			477	β CCC	β OCC(21) + β CCC(22)
A"			463	β CCC	δ HCOC(10) + δ OCCC(15)
A"			408	β CCO	δ HCOC(11)
A'			370	β COC	β OCC(16)
A"			339	δ CCC	δ CCC(10)
A"			279	δ CCC	δ OCCC(10)
A"			248	δ CCC	δ CCC(14)
A'			232	δ CCC	ν OCC(11)+ β OCC(22)
A"			116	δ CCO	δ CCOC(19)+ ν CCCC(16)
A"			106	δ COC	δ CCOC(13) + δ CCCC(11) + δ COCC(50)

ν–stretching; β–in–plane bending; δ–deformation; ρ–rocking; γ–out of plane bending; ω–wagging and τ–torsion. IR and Raman intensities are normalized to 100.

3.5 UV-Visible Analysis

The UV-Visible transitions and its related parameters of 7-hydroxy-4-chromone are computed using B3LYP function and 6-311++G (d,p) basis set along with TD–SCF method. The calculations are performed for both gas and DMSO solvent phases [27]. The experimental UV spectrum is measured in DMSO phase. The calculated and experimental excitation energies, oscillator strength (f) and absorption wavelength (λ) and HOMO–LUMO contributions are presented in Table 6. The UV- theoretical and Experimental spectra are presented in Fig. 8.

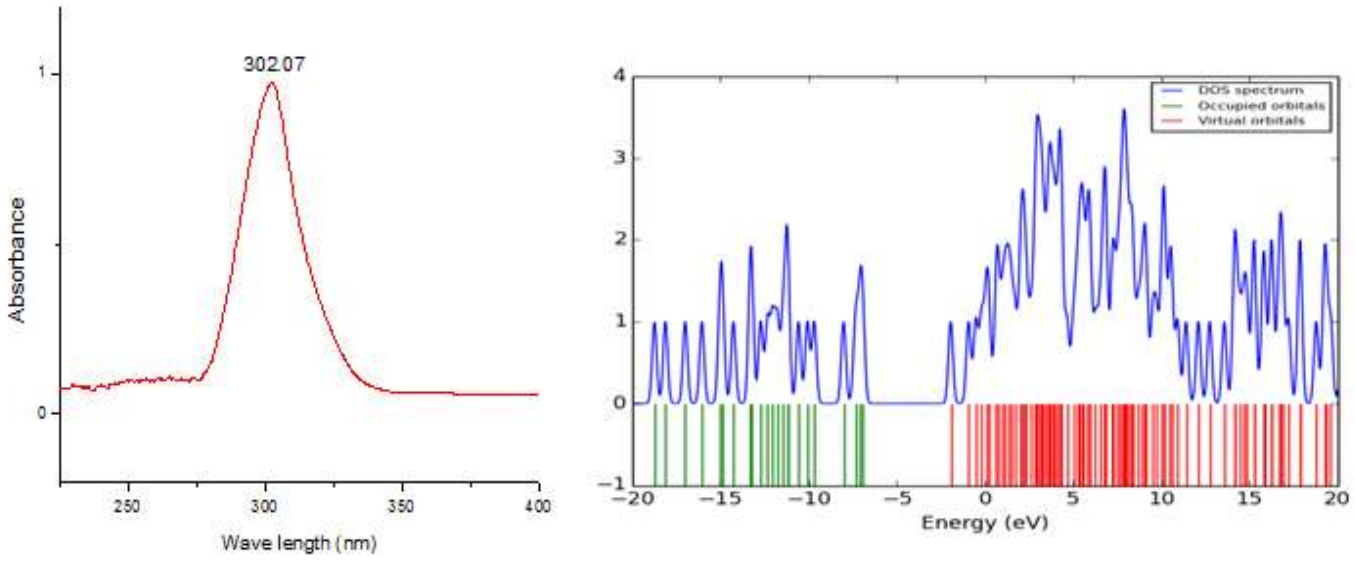

Fig 8: Experimental UV and Dos Spectra of 7-hydroxy 4-chromone

https://doi.org/10.15623/ijret.2018.0702008 Received: 29-12-2017, Accepted: 08-02-2018, Published: 28-02-2018

According to the Table 6, the most probable transitions at DMSO phase have energy gaps 4.0290, 4.4496, 4.5268, eV and their absorption wavelengths are 307.73, 278.64, 277.48, nm respectively, and corresponding oscillator strengths are 0.0000, 0.1991, and 0.0593. The oscillator strength values are the indicator of the absorption coefficient or the intensity of these transitions, the observation of these values indicates that only the transition will have the appreciable intensity of absorption that means only the peak at 277.48 nm wavelengths will be observable in the UV-Vis spectrum. Meanwhile, in case of experimental spectrum it is observed to be around 302.07 nm. According to NBO analysis, the transition which is responsible for this peak is O17 to C1-C2 (n -π*, 30.15 kcal/mol).

The same ten transitions in gas phase have energy gaps, absorption wavelength, oscillator strength are 3.7758, 4.5111, 4.6692 eV and 328.37, 274.84, 265.54 nm and 0.0000, 0.0462, 0.0000 respectively. This observation also illustrates that only the second transition will be visible in the UV-Vis spectrum at wavelength 277.48 nm. The same transition is responsible for this peak O17 to C1-C2 (n -π*, 30.15 kcal/mol). This UV-Vis analysis in different phases shows that there is a variation in the wavelengths of absorption of different peaks which indicate the solvent effect on these electronic transitions.

Table 6: Theoretical electronic absorption spectra of 7-hydroxy-4-chromone (absorption wavelength λ (nm), excitation energies E (ev) and oscillator strengths (f) using TD-DFT/B3LYP/6-311++G(d,p) method.

λ (nm) Theoretical	Experimental	E(eV)	(f)	Major contribution
Gas				
328.37		3.7758	0.0000	H-1->LUMO (96%)
274.84		4.5111	0.1172	HOMO->LUMO (83%)
265.54		4.6692	0.0463	H-2->LUMO (88%)
DMSO				
307.73	302.07	4.0290	0.0000	H-2->LUMO (97%)
277.48		4.4496	0.1991	HOMO->LUMO (88%)
273.89		4.5268	0.0593	H-1->LUMO (86%)

3.6 Homo Lumo Analysis

Frontier molecular orbital (FMO) theory explains the stability of molecular orbital, the distribution of charges at various ground and virtual states and the energy gap between them [28]. The highest occupied molecular orbital (HOMO) and lowest unoccupied molecular orbital (LUMO) are the important molecular orbital's in FMO. These orbital play a major role in governing many chemical reactions and determining electronic band gaps in solids; they are also responsible for the formation of many charge-transfer complexes. The HOMO energy represents the ability of electron giving; LUMO represents the ability of electron accepting; and the energy gap between HOMO and LUMO determines molecular electrical transport properties, chemical reactivity, electrophilic index, hardness and softness of the molecule . Electronegativity (χ) is a measure of the power of an atom or a group of an atom to attract electrons. Global hardness (η) is a measure the resistance of an atom to charge transfer. The global softness (S) describes the capacity of an atom or a group of atoms to receive electrons and is equal to reciprocal of global hardness. The global electrophilicity index (ω) can be calculated from the electronegativity. The energies of highest occupied molecular orbital's (HOMO) and lowest unoccupied molecular orbital (LUMO) are computed with B3LYP function with 6-311++G (d, p) basis set and the pictorial diagram of the HOMO and LUMO is shown in Fig. 9. The HOMO-LUMO energy gap and different reactivity descriptors of molecule in both levels are presented in Table 7.

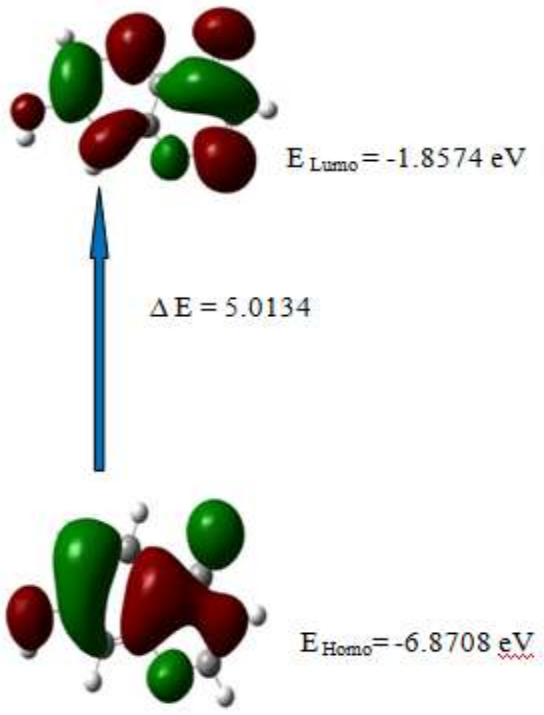

Fig 9: Frontier molecular orbitals of 7-hydroxy 4-chromone

https://doi.org/10.15623/ijret.2018.0702008 Received: 29-12-2017, Accepted: 08-02-2018, Published: 28-02-2018

According to the computed results, 7-hydroxy-4-chromone contains 50 occupied molecular orbitals and 50 unoccupied molecular orbitals. The calculated energy of the HOMO is -6.8708eV and that of LUMO is -1.8574eV. The energy gap between them for Higher Occupied and Lower unoccupied Molecular orbital is -5.0134eV, which shows the possibility of flow of energy from HOMO to LUMO. The electronegativity is a measure of attraction of an atom for electrons in a covalent bond has found to be 4.3641. The global hardness is a measure the resistance of an atom to charge transfer and it is found to be 2.5067. The global softness describes the capacity of an atom or a group of atoms to receive electrons and is equal to reciprocal of global hardness and it is found to be -0.3989. The electrophilicity index is a measure of lowering of total energy due to the maximal electron flow between the donors and the acceptors and it is found to be 3.7989 eV.

Table 7: HOMO, LUMO, Kubo gap, global electronegativity, global hardness and softness, global electrophilicity index of 7-hydroxy 4-chromone.

Parameters	**Gas**
E_{HOMO} (ev)	-6.8708
E_{LUMO} (ev)	-1.8574
$\Delta E_{HOMO\text{-}LUMO\ gap}$ (ev)	-5.0134
Elecronegativity (χ)	4.3641
Global hardness (η)	2.5067
Global softness (S)	-0.3989
Electrophilicity index (ω)	3.7989

3.7 Molecular Electrostatic Potential (MEP) Maps

The molecular electrostatic potential (MEP) surface is a method of mapping electrostatic potential of the rich and poor electron cloud in the molecule. The size and shape of the molecule and dipole moment of the molecule provide a visual method to understand the relative polarity. MEP map also illustrates the charge distributions of molecules three dimensionally. It was computed using B3LYP function with 6-311++G (d, p) basis set [5].The MEP lies in the fact that it simultaneously displays molecular size, shape as well as in case of colour grading, the regions are classified as positive, negative and neutral electrostatic potential and are very useful in research of molecular structure [19]. Potential increases in order of Red<Orange<Yellow<Green<Blue. Blue denotes strongest attraction, Red denotes strongest repulsion and green denotes neutral. In MEPs, the maximum negative region is known as electrophilic reaction, which is depicted in red colour and the maximum positive region is known as nucleophilic reaction, which is depicted in blue colour. The core formed by the naphthalene ring is almost neutral and the edges of the molecule where only Oxygen (15O) atom present possess negative potential, whereas hydrogen atom (18H) lies close to positive potential. The positive and negative potential of the molecule ranges from -7.436 e-2.To7.436 e-2. The values are shown in Fig. 10.

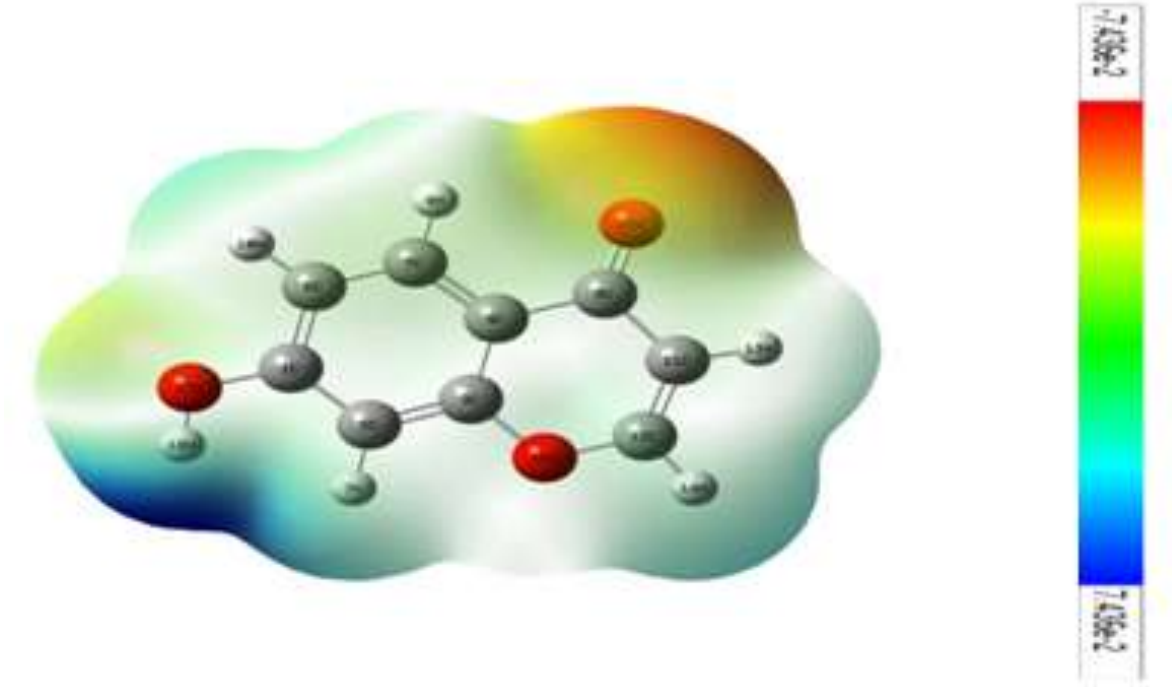

Fig 10: Molecular Electrostatic Potential diagram of 7-hydroxy 4-chromone

https://doi.org/10.15623/ijret.2018.0702008 Received: 29-12-2017, Accepted: 08-02-2018, Published: 28-02-2018

3.8 Docking Study

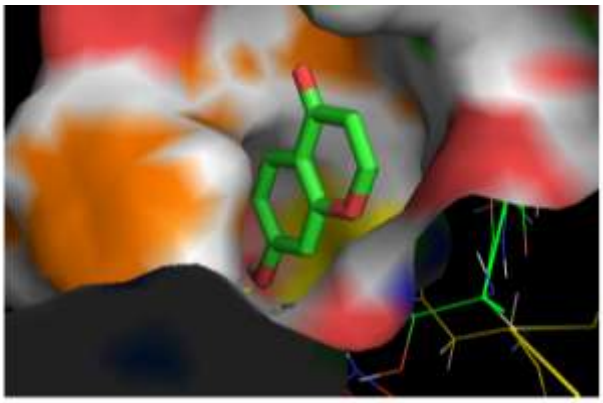

Fig 12 (a): Schematic representation for the docked conformation at active site of the bacterial protein Antimutagenic, (PDB ID 2PYU) along with the title compound MAPE. The active site of the protein is displayed as a surface. Hydrogen bonds are displayed in yellow dotted lines

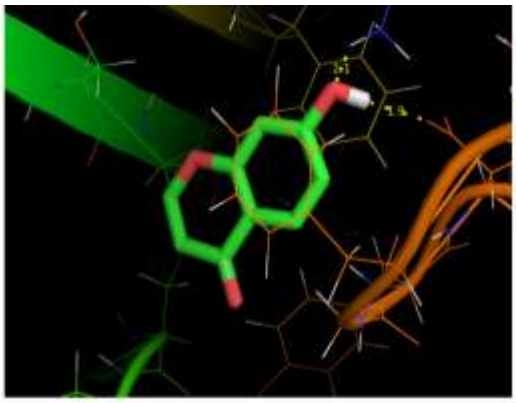

Fig 12 (b): Protein 2PYU with docked ligand in 7-hydroxy 4-chromone

Antimutagenic agents are able to counteract the effects of mutagens. [29]. the interference can be in the form of prevention of the transformation of a mutagenic compound into mutagen, inactivation, or otherwise the prevention of Mutagen-DNA reaction. [30] The antimutagenic potencies also depend on antimutagenic factors, on the mutagenic agent and the tester strain used. The 3D crystal structure of E.coliinosine triphosphate pyrophosphatase RgdB in complex with IMP was obtained from Protein Data Bank (PDB ID: 2PYU). 2PYU has a good resolution 2.02 Å and attached co-crystallized inhibitors were used to identify the active site. Molecular docking is an efficient tool to get an insight into ligand-receptor interactions. All molecular docking calculations were performed on Auto Dock- Vina software [31] and PyMOL molecular graphics systems [32]. The Auto Dock Tools (ADT) graphical user interface was used to calculate Kollmann charges for the protein and to prepare polar hydrogen. Water molecules and co-crystallized ligands were removed. The ligand wasprepared for docking by minimizing its energy at B3LYP/6-311++G (d, p) level of theory. Partial charges were calculated by Gasteiger method. Torsion and rotatable bond were defined. The active site of the enzyme was defined to include residues of the active site within the grid size of 66 Å, 65 Å and 65 Å which are presented in Green color in Fig.12 (a).Lamarckian Genetic Algorithm (LGA) available in Auto Dock-Vina was employed for docking. The docking protocol was tested by removing co-crystallized inhibitor from the protein and then docking it at the same site. To evaluate the quality of docking results, the common way is to calculate the Root Mean Square Deviation (RMSD) between docked pose and the known crystal structure confirmation. This has been depicted in Table 10. RMSD values up to 2.1 Å are considered reliable for docking protocol [33]. The ligand binds at the active site of the protein by H-bonding, which is depicted in yellow dotted lines. GLU-55 of the protein forms hydrogen bonds with –OH group respectively. The inhibitor forms a stable complex with 2PYU as it is obvious from ligand-receptor interactions. Binding free energy (ΔG in kcal/mol) of 1.9 to 2.1 as predicted by Auto-Dock Vina suggests good binding affinity. It is evident that the alcoholic group is crucial for binding. These results draw us to the conclusion that the compound might exhibit inhibitory activity against Antimutagenic and may act as anti-bacterial agent. However, biological tests need to be done to validate the computational predictions Fig.12 (b).Shows the protein 2PYU with docked ligand embedded in the active site and values are tabulated (Table 11).

4. CONCLUSION

In conclusion, the structure of the compound has been determined by using DFT theoretical methods and compared literature values are good agreement. Also the electronic and optical properties of the title compound are also reported using DFT methods. The real and imaginary part of the dielectric function throw light on transitions from occupied to unoccupied bands. In particular charges are predicting drug quality in the molecule. The inhibitor forms a stable complex with 2PYU of E.coliinosine triphospate pyrophoshatase RgdB in comples with IMP as it is obvious from ligand-receptor interactions. Binding free energy (ΔG in kcal/mol) of 1.9 to 2.1 as predicted by Auto-Dock Vina suggests good binding affinity. We hope that our theoretical calculations of the title compound to investigate various properties will be helpful in designing new applications to benefit the society.

ACKNOWLEDGEMENT

We remain grateful to the Department of Physics, St. Joseph's College of Arts and Science (Autonomous), Cuddalore for providing the Quantum Computational Research Lab and Kanchi Mamunivar Center for Post

https://doi.org/10.15623/ijret.2018.0702008 Received: 29-12-2017, Accepted: 08-02-2018, Published: 28-02-2018

Graduates studies, Lawspet for all the Computational works of the Compound and experimental peak for recorded in Pondicherry University for allowing Central Instrumentation Lab and Annamalai University, Chidambaram.

REFERENCES

[1]. I.Sabel, P.G. Fernandes, Electroanalysis (2012) 24, No.3, 618-626.
[2]. J. Liang, Y.X. Tian, L.M. Fu, T.H. Wang,Agr. Food Chem. (2008) 56, 10376.
[3]. J.G. Teixeira, C.B. Dias, D.M. Teixeira, Electroanalysis (2009) 21, 2345.
[4]. A. Aliabadi, F. Shamsa, S. Ostad, Eur J Med. Chem, (2010) 45, 5384.
[5]. S. Sebastian, SpectrochimicaActa Part A: Molecular and Biomolecular Spectroscopy 101 (2013) 370-381.
[6]. M.M. Dias, Food Function, (2011) 2, 595.
[7]. A. Magdy Ibrahim, Journal of Arkivoc (2008) 17, 192-204.
[8]. M. Agostinha, R. Matos, S. Sousa,F. Morais, J. Therm Anal Calorim (2010) 100, 519-526.
[9]. R. Sahan, SalpageJournal of photochemistry and photobiology A: Chemistry 315(2016)14-24.
[10]. Shahriarkhadem, Journal of molecules, 17010191 (2012) 17, 191-206.
[11]. A. Magdy Ibrahim Journal of Arkivoc, (2010) 98-135.
[12]. T.JoselinBeaula, A. Packiavathi et al. SpectrochimicaActa A 138 (2015) 723-735.
[13]. Carthigayan,SpectrochimicaActa Part A : Molecular and Biomolecular Spectroscopy 142 (2015) 350-363.
[14]. P.S. Peek, D.P. Modermoot, SpectrochemicaActa 44 (1988) 371-377.
[15]. M. Kurt,Spectrochemicaacta part A 79(2011) 1162-1170.
[16]. D. Sajan,Spectrochemicaacta part A: Molecular and Biomolecular Spectroscopy (2010).
[17]. M. Govindarajan, SpectrochimcaActa Part A 94 (2012) 53-64.
[18]. M.A. Palafox, J.L. Nunez, M. Gil, J. Mol. Struct. (Theochem) 593 (2002) 101–103.
[19]. A. Altun, K. Golcuk, M. Kumru, J. Mol. Struct. (Theochem.)625 (2003) 17.
[20]. P.B. Nagabalasubramanian, SpectrochimicaActa Part A 85 (2012) 43-52.
[21]. D. R. Leenaraj, Chemical physics letters (2017), 03, 071.
[22]. R. Ditchfield, J. Chem. Phys. 56 (1972) 5688-5691.
[23]. S. Xavier, S. Periandy, S. Ramalingam, SpectrochimicaActa Part A 137 (2015) 306–320)
[24]. S. Manohar, R. Nagalakshmiand V. Krishnakumar, SpectrochimcaActa Part A 71 (2008) 110.
[25]. V. Krishnakumar, R.J. Xavier, Indian J. Pure Appl. Phys. 41 (2003) 597-601.
[26]. M. Karabacak, D. Karagoz, M. Kurt, J. Mol. Struct. 892 (2008) 25–28.
[27]. A.J.D. Melinda, Solid state NMR Spectroscopy; Principles and Applications, Cambridge Press (2003).
[28]. N. Karthikeyan et al. Spectrochimica Acta Part A 139(2015) 229-242
[29]. Karolina Słoczyńska, BeataPowroźnik, ElżbietaPękala, and Anna M. Antimutagenic compounds and their possible mechanisms of action.JAppl Genet.2014; 55(2): 273-285.
[30]. https://en.wikipedia.org/wiki/Antimutagen.
[31]. Oleg Trott, Arthur J. Olson,Journal of Computational Chemistry,31 (2010) 455-461.
[32]. DeLano WL (2002) The PyMOL molecular graphics system, http://www.pymol.org
[33]. B.Kramer, M.Rarey, T.Lengauer, Proteins: Structure, Function and Bioinformatics 37 (1999)228.